

## PAPER

View Article Online  
View Journal | View Issue



Cite this: *Environ. Sci.: Processes Impacts*, 2025, 27, 1088

# Contaminant bioaccessibility in abandoned mine tailings in Namibia changes along a climatic gradient†

Vojtěch Ettler, <sup>a\*</sup> Tereza Křížová, <sup>a</sup> Martin Mihaljevič, <sup>a</sup> Petr Drahota, <sup>a</sup> Martin Racek, <sup>b</sup> Bohdan Kříbek, <sup>c</sup> Aleš Vaněk, <sup>d</sup> Vít Penížek, <sup>d</sup> Tereza Zádorová, <sup>d</sup> Ondra Sracek <sup>e</sup> and Ben Mapani <sup>f</sup>

Fine-grained dust from tailing storage facilities in abandoned sulfide-ore mining areas represents an important source of environmental contamination. Fine fractions (<48  $\mu\text{m}$  and <10  $\mu\text{m}$ ) of tailings from three old mining sites situated along a climatic gradient from hot semiarid to cold desert conditions in Namibia were studied: Kombat (Cu–Pb–Zn; rainfall  $\sim 500$  mm), Oamites (Cu;  $\sim 120$  mm), Namib Lead & Zinc (Pb–Zn;  $\sim 0$  mm). Multi-method mineralogical and geochemical investigations were adopted to assess the binding and gastric bioaccessibility of the metal(loid)s and to evaluate the associated human health risks. The total concentrations of contaminants in the tailings generally increased with the decreasing particle size (up to 134 mg As  $\text{kg}^{-1}$ , 14 900 mg Cu  $\text{kg}^{-1}$ , 8880 mg Pb  $\text{kg}^{-1}$ , 13 300 mg Zn  $\text{kg}^{-1}$ ). The mean bioaccessible fractions varied substantially between the sites and were significantly higher for the tailings from the sites with a higher rainfall (73–82% versus 22%). The mineralogical composition of the tailings, reflecting the original mineralogy and the degree of the weathering process, is the main driver controlling the bioaccessibility of the metal(loid)s. In desert environments, metal(loid)s in tailings are bound in sulfides or sequestered in secondary Fe oxyhydroxides and/or Fe hydroxysulfates, all of which are insoluble in simulated gastric fluid. In contrast, tailings from areas with higher precipitation contain metal(loid)s hosted in carbonate phases (malachite, cerussite), which are highly soluble under gastric conditions. Based on the higher contaminant bioaccessibility, the vicinity of the settlement and farmlands, and a higher percentage of wind-erodible fine particles, a higher risk for human health has thus been identified for the Kombat site, where further remediation of the existing tailings storage facility is highly recommended.

Received 24th January 2025  
Accepted 19th March 2025

DOI: 10.1039/d5em00060b

rsc.li/epsi

## Environmental significance

Wind-blown fine dust from tailings storage facilities represents an important source of metal(loid)s with numerous environmental and health consequences. Our multi-method characterization approach adopted on fine particle-size fractions of abandoned tailings situated along a climatic gradient in Namibia indicates that the oral bioaccessibilities of metal(loid)s were substantially lower under desert conditions due to efficient sequestration in the minerals persistent in the simulated gastric fluid (sulfides, Fe oxyhydroxides, and Fe hydroxysulfates). In contrast, tailings from semiarid areas with higher rainfall weathered more, and metal(loid)s were hosted in highly soluble carbonates readily dissolved under gastric conditions. The risk for local communities is thus substantially higher in semiarid areas, pointing out the need for environment-friendly remediation.

<sup>a</sup>Institute of Geochemistry, Mineralogy and Mineral Resources, Faculty of Science, Charles University, Albertov 6, 128 00 Prague 2, Czech Republic. E-mail: ettler@natur.cuni.cz

<sup>b</sup>Institute of Petrology and Structural Geology, Faculty of Science, Charles University, Albertov 6, 128 00 Prague, 2, Czech Republic

<sup>c</sup>Czech Geological Survey, Geologická 6, 152 00 Prague 5, Czech Republic

<sup>d</sup>Department of Soil Science and Soil Protection, Faculty of Agrobiological, Food and Natural Resources, Czech University of Life Sciences Prague, Kamýcká 129, 165 00 Prague 6, Czech Republic

<sup>e</sup>Department of Geology, Faculty of Science, Palacký University in Olomouc, 17. listopadu 12, 771 46 Olomouc, Czech Republic

<sup>f</sup>Department of Civil, Mining and Process Engineering, Namibia University of Science and Technology, Windhoek, Namibia

† Electronic supplementary information (ESI) available: Contains 9 tables and 7 figures with basic characteristics and the mining history of the sampling sites, description of the tailings, QC/QA and analytical conditions, XRD results, SEM-EPMA results, total and bioaccessible concentrations and results of the exposure calculations. See DOI: <https://doi.org/10.1039/d5em00060b>



# 1. Introduction

Dust particles from mining operations and waste storage facilities are considered a source of environmental contamination.<sup>1,2</sup> Dry conditions, incomplete vegetation cover, and strong winds in mining areas are responsible for the dispersion of dust particles, which can travel large distances. Recent investigations from copper mining areas in the Atacama Desert in Chile demonstrated that an alarming situation is generally observed within 20 km downwind of the mining sites; however, some metal(loid)-bearing dust travels up to 70 km away.<sup>3</sup> Mining-derived dust particles may have a direct effect on quality of soils and crops<sup>4–9</sup> and represent a health risk for communities working and living nearby.<sup>10–18</sup>

The mineral industry of Africa is the second-largest in the world, yet the human health impacts of mining and ore-processing activities remain largely underexplored, particularly in sub-Saharan Africa. Only a few exposure studies based on biomarkers (blood, urine, feces, toenails) have been carried out so far; for instance, in the Co–Cu mining district of Katanga, the Democratic Republic of the Congo (DRC),<sup>19–21</sup> the Cu mine area in Kilembe, Uganda,<sup>22</sup> the Pb–Zn mining areas of Kabwe, Zambia,<sup>23</sup> and Nasawara, Nigeria.<sup>24</sup> Bioaccessibility investigations in mining areas of Africa have been increasingly adopted during the last fifteen years on contaminated soils<sup>16,25</sup> and dust from mining and ore-processing technologies<sup>14–17,26–28</sup> to assess any potential risks for human health. Unfortunately, the number of studies is still very limited in Namibia, which is experiencing the long-term legacy of the mining industry.<sup>29</sup> Most risk assessments have been based on the total contaminant concentrations, comparisons with limits for soils, and the wind dispersion of the contaminated dust particles near abandoned mining sites.<sup>4,5,30–33</sup> In a pioneering study from abandoned and active mining and smelting areas in northern Namibia, Ettler *et al.*<sup>14</sup> compared the contaminant oral bioaccessibilities in the dust of various origins and found that compared to mine tailings, slags and smelter dust exhibited substantially higher contaminant extractability under gastric conditions where, especially, As, Pb and Cd grossly exceeded the tolerable daily intakes. More recently, a relatively low health risk was documented from a mining and hydrometallurgical operation processing non-sulfide Zn ores operating in the arid environment of southern Namibia; the authors concluded that the safety measures required by the mine operator helped to prevent the staff's exposure from dust-derived contaminants.<sup>17</sup>

The primary mineralogical and geochemical compositions of the tailings affect their evolution in disposal sites. The climate, precipitation rate and corresponding relative humidity (RH) in the tailings are also important factors influencing the compositional changes of the tailings over time. A recent experimental study on the stability of arsenopyrite (FeAsS) and löllingite (FeAs<sub>2</sub>), representing the most common As minerals in the waste produced by mining and ore processing activities, indicated that the increasing RH significantly increased the oxidation rate of both minerals.<sup>34</sup> The analysis of pyrite grains in the tailings revealed their greater oxidation/dissolution in

a semiarid climate over an arid climate in northern Chile underlining the effects of the climate on mineralogical transformations.<sup>35</sup> Also, based on a study from high-arsenic mine waste in New Zealand, there is evidence that more soluble secondary phases form during the long-term exposure of tailings exposed to humid environments compared to dryer climates.<sup>36</sup>

Several studies have suggested that weathering may change the contaminant bioaccessibility in mine tailings and dust emissions from tailings storage facilities.<sup>37–39</sup> The question arises to which extent the contaminant bioaccessibility is also affected by contrasting climates. To expand our knowledge about the risk related to dust samples from large tailings storage facilities and to better understand the relationship between climate and metal(loid)s bioaccessibility, this study focuses on three former (50–60 years old) metal-mining sites in Namibia situated along a climatic gradient. Namibia is a relatively dry country with climatic conditions varying from the savanna-type semiarid environments in the north to (hyper)arid environments in the south and around the Atlantic coast.<sup>40,41</sup> The three study sites are situated in contrasting climatic settings (ranging from hot semiarid conditions with an annual precipitation of ~500 mm to cold desert conditions with practically no precipitation; Fig. S1 in the ESI†) and provide a unique opportunity to explore the long-term climatic effects on the tailings' geochemical and mineralogical characteristics, contaminant bioaccessibility and potential influence on human health.

## 2. Materials and methods

### 2.1 Study areas

Kombat is situated in the Otavi Mountainland in the Otjozondjupa region in northeastern Namibia (Fig. 1a). The carbonate-hosted Cu–Pb–Zn–Ag mineralization was exploited mainly between 1962 and 2008 when the mine was closed due to flooding. From 2021, the mine is owned by the Canadian company Trigon Metals. Production from the open pit recommenced in 2023 by mining the Cu ore with a 1.2% average grade and re-opening the underground mining activities is planned (for details, see the ESI†). More than 300 Mt of tailings were deposited in a tailings dam (Fig. 1b and S2a†), which is regarded as a source of environmental contamination for farmland soils and ecosystems<sup>42,43</sup> (see the ESI† for other studies).

The Oamites mine site is situated approximately 50 km south of Windhoek, the capital of Namibia, in the Khomas region in central Namibia (Fig. 1a). The mine was productive between 1971 and 1984 and extracted mostly Cu sulfide ores (Cu grade of 1.33%). The operation produced approximately 5.5 Mt of tailings deposited in two storage facilities, which were highly affected by wind erosion and situated near a large military base (Fig. 1c and S2b,† for details, see the ESI†).<sup>32,33</sup>

The Namib Lead & Zinc mine is located in the Rössing Mountain Area, in the Erongo region in western Namibia (Fig. 1a). This sulfidic Pb–Zn deposit was mined from 1968 to 1991, and the mining and ore processing activities were renewed between 2019 and 2020. The mine has currently been



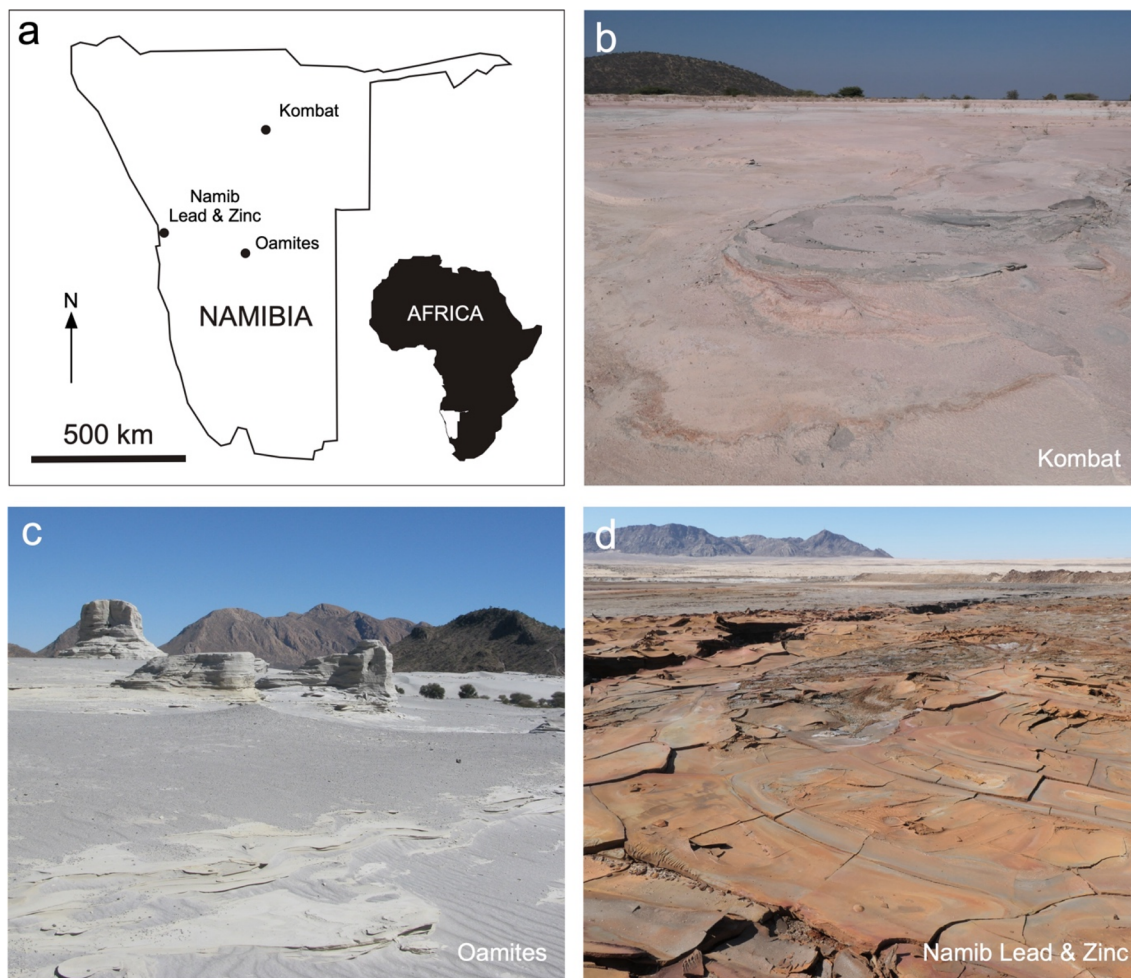


Fig. 1 Location (a) and photographs of the tailings disposal sites at the studied sites: Kombat (b), Oamites (c), and Namib Lead & Zinc (d).

placed under care and maintenance. Two tailings storage facilities are located southeast of the mine area (Fig. 1 and S2c; for details, see the ESI†).

The three study sites are situated along a significant climatic (and rainfall) gradient (Fig. S1†). Whereas the Kombat site experiences a hot semi-arid climate (“Bsw” according to the Köppen–Geiger classification),<sup>44</sup> the Oamites and Namib Lead & Zinc sites correspond to a cold desert climate (“Bwh” according to the Köppen–Geiger classification). According to the World Bank’s Climate Change Knowledge Portal, the mean annual temperatures and precipitation for the studied regions are highly variable: the Otjozondjupa region (Kombat): 21.5 °C, 417 mm; the Khomas region (Oamites): 20.5 °C, 279 mm; the Erongo region (Namib Lead & Zinc): 20.2 °C, 136 mm.<sup>45</sup> However, the latter site is characterized by the extreme aridity of the Namib Desert, and the annual rainfall is generally <25 mm with years of no rain at all (*cf.* Fig. S1†).<sup>46</sup> The annual precipitation rates recorded for 2023 by nearby measuring stations were as follows: Kombat 499 mm, Rehoboth (20 km S of Oamites) 122 mm, Rössing Village (15 km SSE of Namib Lead & Zinc) 0 mm (<https://www.MeteoBlue.com>). Dry conditions and strong winds (Fig. S1 and S3†) are responsible for the aeolian

erosion of the tailings disposal sites and the dispersion of dust particles into the surrounding environment (Fig. 1).<sup>29</sup> Such risk is exceptionally high for Kombat, where farmlands and settlements are located downwind, and for Oamites with a military base located SE of the tailings storage facilities, *i.e.*, downwind of the strongest northwesterly winds (Fig. S2 and S3†).

## 2.2 Sampling and processing of tailings

For the collection of tailings, we used the EuroGeoSurveys methodology used for soil collection based on a 10 × 10 m grid to collect five subsamples (in each corner and the center of this square) to obtain one composite sample per spot.<sup>47</sup> At each spot, a sample of the surface tailings material weighing approximately 2 kg (maximum depth: 5–10 cm) was collected using a plastic shovel (Fiskars, Finland). In total, two samples were collected at each studied site, resulting in six composite samples from six different tailing facilities. The GPS coordinates and basic descriptions of the individual samples are reported in Table S1.†

The tailings were freeze-dried, and the entire samples were passed through a 2 mm stainless steel sieve (Retsch, Germany),





indicating that the material underwent the comminution step before flotation. The original tailings were further sieved to <48  $\mu\text{m}$ , a fraction recommended in many studies as adhering to surfaces on hands leading to accidental ingestion through hand-to-mouth behavior.<sup>48</sup> To conform with our previous investigations,<sup>15–17</sup> we performed additional sieving to <10  $\mu\text{m}$ , a dust fraction entering the lung compartment, but mostly expelled by the rapid clearance of the upper airways (nasopharynx) *via* the mucociliary escalator, swallowed and subsequently transported into the gastrointestinal tract (only particles smaller than  $\sim 3 \mu\text{m}$  may enter the deep lung).<sup>49,50</sup> The <48  $\mu\text{m}$  and <10  $\mu\text{m}$  fractions were obtained by dry sieving using a UHELON 120T 48  $\mu\text{m}$  polyamide sieve (Silk & Progress, Brn  nec, Czech Republic) and a SEFAR NITEX 03-10/2 10  $\mu\text{m}$  polyamide sieve (SEFAR AG, Switzerland), respectively. Aliquots of each sample (original tailings, <48  $\mu\text{m}$ , and <10  $\mu\text{m}$  fractions) for determining the total elemental concentrations and phase compositions were further pulverized in an agate mortar (Retsch planetary mill PM 400, Germany).

### 2.3 Tailings dust characterization

The pH of the original tailings samples was measured in deionized water according to the ISO 10390 method (1 : 5 solid-to-liquid ratio, 5 min vigorous agitation followed by 2 h decantation).<sup>51</sup> A WTW Multi 3620 IDS pH meter equipped with a WTW Sentix 940 pH electrode calibrated against WTW technical buffers 4.01, and 7.00 was used (WTW, Germany).

The bulk chemical compositions of the solid samples were determined after digestion in acids. A mass of 0.2 g of each material (original tailings, <48  $\mu\text{m}$ , and <10  $\mu\text{m}$  fractions) was decomposed using a hot acid mixture (9 ml of concentrated  $\text{HNO}_3$  and 3 ml of concentrated  $\text{HF}$ ; Merck Ultrapure, Germany) in a microwave unit (Multiwave 5000, Anton Paar, Austria). The dissolved sample was transferred into polytetrafluoroethylene (PTFE) beakers (Savillex, USA) and evaporated on a hot plate. The solution residuum was dissolved in 2%  $\text{HNO}_3$  (v/v) and analyzed by a combination of inductively coupled plasma optical emission spectrometry (ICP-OES; Agilent 5110, USA) and quadrupole-based inductively coupled plasma mass spectrometry (ICP-MS, Thermo Scientific iCAP-Q<sup>TM</sup>, Germany). The major elements and selected metals (Al, Ca, Cu, Fe, K, Mg, Mn, Pb, S, Ti, and Zn) were determined by ICP-OES, and the trace elements (Ag, As, Cd, Cr, Ni, Sb, and V) were determined by ICP-MS. A quality control/quality assurance (QC/QA) procedure was carried out by the parallel digestion and analysis of standard reference materials (SRMs) 2710a (Montana I Soil) and 2711a (Montana II soil) released by the National Institute of Standards and Technology (NIST, USA). The recoveries of individual elements were found to be satisfactory (Table S2<sup>†</sup>).

The mineral phase composition of the tailings was determined by X-ray diffraction (XRD) analysis using a PANalytical X'Pert Pro diffractometer (PANalytical, the Netherlands) with an X'Celerator detector ( $\text{CuK}\alpha$  radiation at 40 kV and 30 mA, 2 theta range of 2–80 $^\circ$ , step of 0.02 $^\circ$ , counting time of 150 s per step). The obtained diffraction patterns were processed using the X'Pert HighScore Plus 3.0 software coupled with the

Crystallography Open Database (COD).<sup>52</sup> The <48  $\mu\text{m}$  dust fractions were prepared as polished sections and examined by an electron probe microanalyzer (EPMA; JEOL JXA-8530F, Japan) equipped with a field emission gun (FEG) electron source and a JEOL JED-2300F energy dispersion spectrometer (EDS). The same instrument was used for the scanning electron microscopic (SEM) imaging, EDS analyses, and quantitative chemical analyses of individual minerals using wavelength dispersion spectroscopy (WDS). The detailed analytical conditions, standards, and detection limits for the EPMA measurements are given in Table S3<sup>†</sup>.

### 2.4 Bioaccessibility testing and exposure assessment

The oral bioaccessibility test, corresponding to a gastric phase extraction, was performed according to the US Environmental Protection Agency's (EPA's) experimental protocol (2017).<sup>53</sup> The original tailings and the sieved tailings dust fractions were extracted in a simulated gastric fluid (SGF) composed of a 0.4 M glycine solution adjusted to  $\text{pH } 1.5 \pm 0.05$  by  $\text{HCl}$  (reagent grade, Merck, Germany) at a liquid-to-solid (L/S) ratio of 100 (0.1 g of soil to 10 ml of extracting solution). The mixtures were agitated for 1 h at 37  $^\circ\text{C}$  in a GFL 3032 incubator (GFL, Germany). The extractions were performed with procedural blanks and in duplicate for the original tailings and <48  $\mu\text{m}$  dust fractions, while the <10  $\mu\text{m}$  fractions were extracted only once due to the limited sample amounts. The extracts were syringe-filtered through a 0.45  $\mu\text{m}$  membrane filter (using Millex-HV PVDF Durapore, Millipore, USA). The pH and redox potential values were immediately measured using a WTW Multi 3620 IDS multimeter equipped with a WTW SenTix<sup>®</sup> 940 pH electrode and a SenTix<sup>®</sup> ORP-T 900 redox electrode (WTW, Germany). The instrument was calibrated and verified using WTW technical pH buffers (2.00, 4.01, and 7.00) and a WTW RH28 redox standard (220 mV for  $\text{Pt-Ag/AgCl}$  at 25  $^\circ\text{C}$ ). The solutions obtained were then diluted in 2%  $\text{HNO}_3$  (v/v) and analyzed by ICP-OES and/or ICP-MS for the following elements: Ag, Al, As, Ca, Cd, Cr, Cu, Fe, Mg, Mn, Ni, Pb, S, Sb, Si, V, and Zn. The bioaccessible concentrations of the metal(loid)s were expressed in  $\text{mg kg}^{-1}$  and converted to a bioaccessible fraction (BAF; percentage of the total contents).

The NIST SRMs 1463f (trace elements in water) and 1640a (trace elements in natural water) were used to verify the accuracy of the ICP measurements in the extracts (Table S2<sup>†</sup>). Furthermore, to verify the accuracy of the bioaccessible extraction, NIST SRM 2710a and 2711a were extracted using the SGF, and the bioaccessible concentrations of Pb and As were compared with the certified and published values (Table S4<sup>†</sup>).<sup>53,54</sup>

The exposure estimates were calculated for children (weighing 10 kg) and adults (weighing 70 kg), being considered as potential target groups, even though only in Kombat, where settlements are close to the tailings storage facility, children can be in direct contact with the contaminated dust. The soil and dust ingestion rates are somewhat variable, and the conservative daily soil/dust intake used as a model in this type of exposure assessment generally corresponds to 50 mg per day for adults and 100 mg per day for children.<sup>26,55</sup> It has nevertheless been demonstrated that the dust ingestion rates in the mining



areas of sub-Saharan Africa could be much higher. For instance, Smolders *et al.*<sup>21</sup> indicated that in Cu–Co mining areas of the Democratic Republic of Congo, the dust ingestion rates corresponded to 280 mg per day (geometric mean for all the data set) and 1700 mg per day (average value for children, age 4–15 years). Thus, apart from the conservative value (100 mg per day), we also compared exposures when a higher dust ingestion rate of 280 mg per day was considered. Minimal risk levels (MRLs) defined by the US Agency for Toxic Substances and Disease Registry (ATSDR)<sup>56</sup> were primarily used for the exposure assessment ( $\mu\text{g per kg}_{\text{bw}}$  per day, exposure duration) (bw = body weight): As (5, acute; 0.3, chronic), Cd (0.5, intermediate; 0.1 chronic),  $\text{Cr}^{\text{VI}}$  (5, intermediate; 0.9 chronic), Cu (20, acute/intermediate; recently increased from 10 to 20), V (10, intermediate), and Zn (300, intermediate/chronic). Furthermore, the obtained daily intakes of metal(oid)s were also compared with the tolerable daily intake (TDI) limits taken from Baars *et al.*<sup>57</sup> and Tiesjema and Baars,<sup>58</sup> especially in the case of the contaminant's absence in the ATSDR list ( $\mu\text{g per kg}_{\text{bw}}$  per day): As (1), Cd (0.5),  $\text{Cr}^{\text{VI}}$  (5), Cu (140), Ni (50), Pb (3.6), V (2), and Zn (500). It has to be noted that compared to the latter TDI values, the European Food Safety Authority (EFSA) has a lower TDI for Cd corresponding to  $0.36 \mu\text{g kg}_{\text{bw}}^{-1}$ ,<sup>59</sup> for Ni corresponding to  $2.8 \mu\text{g kg}_{\text{bw}}^{-1}$  (ref. 60) and suggested that the provisional TDI limit for Pb ( $3.6 \mu\text{g kg}_{\text{bw}}^{-1}$ )<sup>61</sup> and As ( $2.14 \mu\text{g kg}_{\text{bw}}^{-1}$ )<sup>62</sup> are no longer appropriate due to their toxicity. Moreover, US EPA reference dose limits (RfD)<sup>63</sup> were also used for comparison purposes (Table S9†), especially for Ag, which was not listed in the previously mentioned databases.

## 2.5 Data processing and geochemical modeling

The obtained data were processed and plotted using a combination of the Prism 10 (GraphPad, USA) and Graphic for Mac (Picta, USA) software packages. Prism 10 was also used for the statistical data treatment. The normality of data was assessed using the Shapiro–Wilk or Kolmogorov–Smirnov test ( $\alpha = 0.05$ ). A one-way analysis of variance (ANOVA) was performed to evaluate the statistical differences between the chemical compositions and the bioaccessible concentrations in the individual tailings dust fractions. Friedman's test and Dunn's multiple comparison test ( $\alpha = 0.05$ ) were adopted for the data with lognormal distribution, and Tukey's multiple comparison test ( $\alpha = 0.05$ ) was used for the data with normal distribution. The geochemical code PHREEQC-3 for macOS<sup>64</sup> was used for the equilibrium speciation-solubility modeling to calculate the elemental speciation and the degree of saturation of the bioaccessibility extracts with respect to the potential solubility-controlling phases (*i.e.*, the calculation of the saturation index,  $\text{ESI}^\dagger$ ). The minteq.v4.dat thermodynamic database was used for all the calculations.

## 3. Results

### 3.1 Characterization and composition of the tailings

Tailings from the three study sites (K – Kombat, O – Oamites, N – Namib Lead & Zinc) exhibited variable granulometries.

Whereas for the K samples, the  $<48 \mu\text{m}$  fraction accounted for 50–82% of the original sample, the other sites exhibited a lower percentage of the fine fraction (10–34% of the original sample). Interestingly, the O samples contained a significantly higher percentage of the  $<10 \mu\text{m}$  fraction (3.3–4.7%) compared to the other sites ( $<0.5\%$  of the original sample) (Table S1†). The equilibrium pH measured on the original tailings was alkaline for the K and O samples (8.3–8.7) and slightly acidic for the N samples (6.0–6.3) (Table S1†).

The contrasting color of the samples reflects the mineralogical composition of the tailings. The K tailings are white or grey (K1) with pinkish and pale red tones (K2) (Fig. 1 and Table S1†) and are primarily composed of carbonates [calcite,  $\text{CaCO}_3$ , and dolomite,  $\text{CaMg}(\text{CO}_3)_2$ ] with less abundant micas and quartz and minor-to-trace amounts of efflorescence salts (gypsum,  $\text{CaSO}_4 \cdot 2\text{H}_2\text{O}$ ; hexahydrate,  $\text{MgSO}_4 \cdot 6\text{H}_2\text{O}$ ), Fe (oxyhydr)oxides (goethite,  $\text{FeOOH}$  and hematite,  $\text{Fe}_2\text{O}_3$ ) and malachite [ $\text{Cu}_2(\text{CO}_3)(\text{OH})_2$ ] (Table S5†). The O tailings are light grey and mostly contain quartz, micas, and feldspars (Fig. 1; Tables S1 and S5†). The N tailings exhibit rusty-to-red colors (Fig. 1 and Table S1†) and apart from major gypsum and common-to-minor quartz, micas, and carbonates, the XRD confirmed the presence of various Fe (oxyhydr)oxides (goethite, lepidocrocite), siderite ( $\text{FeCO}_3$ ) and numerous sulfides (pyrite,  $\text{FeS}_2$ , pyrrhotite,  $\text{Fe}_{1-x}\text{S}$  and sphalerite,  $\text{ZnS}$ ) (Table S5†). Soluble salts (*e.g.*, halite,  $\text{NaCl}$ ) and native sulfur were also found by XRD in samples N1 and N2, respectively (Table S5†).

Using a combination of SEM/EDS and EPMA, we gained a better insight into the metal(loid) contaminants binding and their distribution within the individual minerals (Fig. 2, Tables S6 and S7†). The K samples contain only rare sulfides (*e.g.*, tiny grains of chalcopyrite,  $\text{CuFeS}_2$ ), and metals are mainly hosted in secondary phases. Malachite,  $\text{Cu}_2(\text{CO}_3)(\text{OH})_2$ , is a key Cu-bearing phase, but Cu was also detected in other phases, such as Fe (oxyhydr)oxides (FOH; up to 0.38 wt%) and complex phase mixtures (see the unidentified Pb–Fe–Cu phase in Fig. 2a and the EPMA analysis in Table S7,† spot 4). Low Cu concentrations were also found in the hematite ( $\text{Fe}_2\text{O}_3$ ; 0.07 wt% CuO) and primary carbonates (0.06 wt% CuO) (Fig. 2a and Table S7†). The major hosts of Pb are Fe (oxyhydr)oxides (up to 11.8 wt% PbO), unidentified complex phase mixtures (up to 31.7 wt% PbO), and tiny cerussite ( $\text{PbCO}_3$ )-like crystals, too small to be analyzed by EPMA (Fig. S4a†). Lead was also detected in gangue minerals (calcite), hematite, and malachite but generally at concentrations  $<0.2 \text{ wt}\%$  PbO (Table S7†). Zinc is primarily bound in Fe (oxyhydr)oxides (2.5 wt% ZnO) and carbonates (siderite,  $\text{FeCO}_3$ ; 6.8 wt% ZnO) (Table S7†). Other minor contaminants were not detected in the K tailings except for low As concentrations in some Fe (oxyhydr)oxides and unidentified complex mixtures (up to 0.11 wt%  $\text{As}_2\text{O}_5$ ) (Table S7†).

The O tailings contain residual grains of sulfides partly weathered to Fe (oxyhydr)oxides. Copper is mainly hosted in residual chalcopyrite, the major extracted mineral at this site (Fig. 1c), but low amounts of Cu were also recorded in pyrrhotite ( $\text{Fe}_{1-x}\text{S}$ ; 1.08 wt%) and pyrite ( $\text{FeS}_2$ ; 0.04 wt%) (Fig. 1d and Table S6†). Additionally, pyrrhotite was also found to contain Ag- and Ni-bearing submicrometric inclusions analyzed by EDS



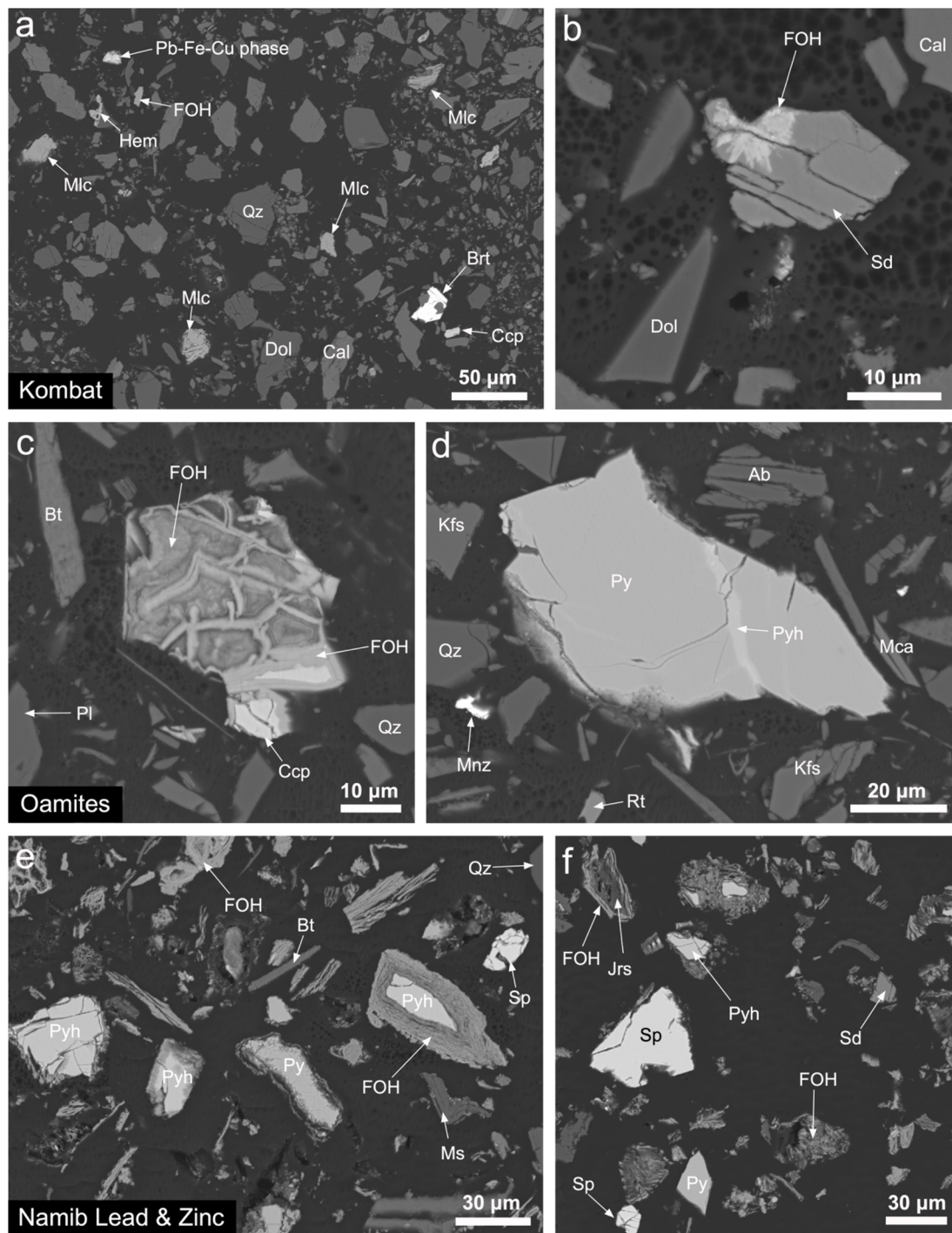


**Fig. 2** Scanning electron micrographs of the <48  $\mu\text{m}$  fraction of the tailings from Kombat (a and b), Oamites (c and d), and Namib Lead & Zinc (e and f) (in back-scattered electrons, BSE). (a) General view of the gangue grains composed of quartz, dolomite, and calcite associated with abundant malachite, metal-bearing Fe (oxyhydr)oxides and hematite, complex mixtures (Pb–Fe–Cu phase) and rare barite; (b) Crystals of metal-bearing Fe (oxyhydr)oxides embedded in siderite and associated with calcite and dolomite; (c) weathered chalcopyrite grain with the alteration rim composed of metal-bearing Fe (oxyhydr)oxides and associated with gangue minerals (quartz, biotite, plagioclase); (d) primary sulfide grain composed of pyrite and pyrrhotite in association with fragments of gangue minerals (quartz, feldspars, mica, rutile, monazite); (e) sulfide grains (pyrrhotite, pyrite, sphalerite), some of them highly weathered with rims of Fe (oxyhydr)oxides associated to gangue minerals (quartz, micas); (f) sphalerite, pyrite and pyrrhotite grains associated to siderite and secondary Fe (oxyhydr)oxides and jarosite. Mineral abbreviations according to Warr:<sup>65</sup> Ab – albite, Brt – barite, Bt – biotite, Cal – calcite, Ccp – chalcopyrite, Dol – dolomite, FOH – Fe (oxyhydr)oxide, Hem – hematite, Jrs – jarosite, Kfs – K-feldspar, Mca – mica, Mlc – malachite, Mnz – monazite, Qz – quartz, Pl – plagioclase, Py – pyrite, Pyh – pyrrhotite, Rt – rutile, Sd – siderite, Sp – sphalerite.





(Fig. S4b†). Original sulfide ore mineralization also contained some native Ag grains and veins.<sup>66</sup> However, these were probably efficiently extracted from the ore during flotation and are thus absent in the tailing. Secondary Fe (oxyhydr)oxides forming rims around the altered sulfides in the tailings also contain metals (17.1 wt% Cu, 7.2 wt% Pb, 1.2 wt% Zn) (Table S7†).

Arsenic and other trace contaminants in the minerals of O tailings were below the detection limits.

Compared to the other sites, the N tailings were the most enriched in metal sulfides (Fig. 2e and f). Sphalerite (ZnS) was the major Zn-hosting phase in the tailings, but about 0.07 wt% Zn was also detected in pyrite and pyrrhotite (Table S6†), Fe

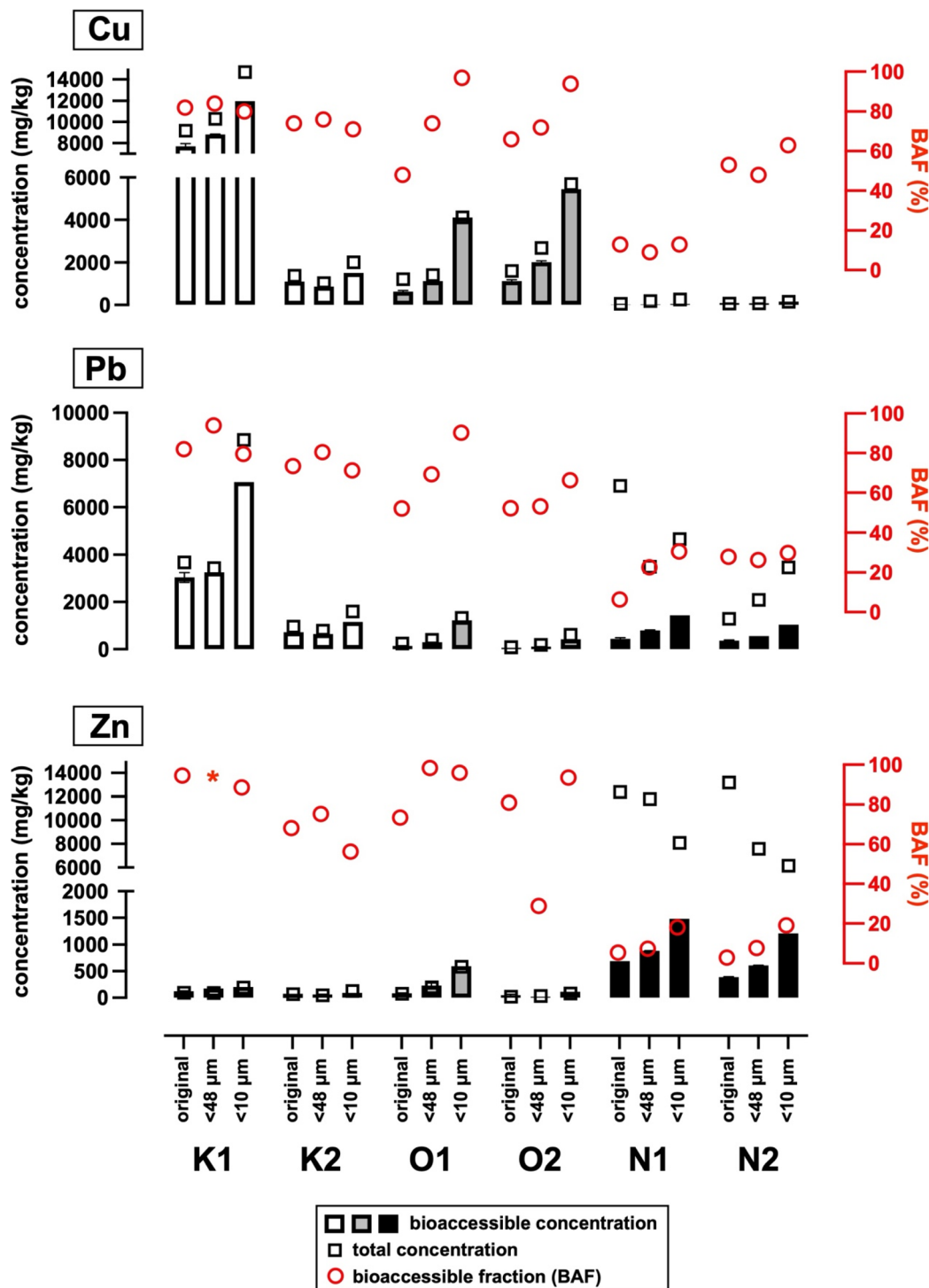


Fig. 3 Total concentrations (squares), bioaccessible concentrations (bars), and bioaccessible fractions (red dots) of Cu, Pb, and Zn in the original tailings and the <48 μm and the <10 μm fractions of the tailings. Asterisk indicates an outlier BAF value for Zn, exceeding 100%, probably related to the "nugget effect" and/or sample inhomogeneity. Symbols for the individual sites: K = Kombat, O = Oamites, N = Namib Lead & Zinc.



(oxyhydr)oxides and the jarosite group minerals [(K, Na, Pb, H<sub>3</sub>O) Fe<sub>3</sub>(SO<sub>4</sub>)<sub>2</sub>(OH)<sub>6</sub>; up to 0.38 wt% ZnO; Table S7†]. No specific Pb minerals were recorded, but this metal was partitioned among the sulfides (<0.19 wt% Pb) and secondary weathering products [Fe (oxyhydr)oxides, jarosite] (Tables S6 and S7†). The latter secondary minerals also contained low concentrations of Ni, As, and Cu (generally <0.1 wt% oxide); the other contaminants were below their detection limits (Table S7†).

The bulk chemical data indicate that the concentrations of the studied contaminants (Ag, As, Cd, Cr, Cu, Ni, Pb, Sb, V, and Zn) (Table S8†) varied between sites and particle size fractions. Copper, Pb, and Zn are the most abundant contaminants (Cu: 158–14 900 mg kg<sup>-1</sup>; Pb: 115–8880 mg kg<sup>-1</sup>; Zn: 60.0–13 300 mg kg<sup>-1</sup>). Other trace elements were found in much lower concentrations (Ag: 1.0–22.7 mg kg<sup>-1</sup>; As: 2.0–134 mg kg<sup>-1</sup>; Cd: 0.2–48.6 mg kg<sup>-1</sup>; Cr: 8.4–704 mg kg<sup>-1</sup>; Ni: 3.4–92.4 mg kg<sup>-1</sup>; Sb: 0.6–16.5 mg kg<sup>-1</sup>; V: 10.9–355 mg kg<sup>-1</sup>). The differences between individual sites correspond well to the types of mined ores. Whereas the N tailings are enriched in Zn, higher concentrations of Cu were observed in the K and O tailings, and Pb occurred to a higher extent in the K and N tailings (Fig. 3 and Table S8†). Generally, the concentrations of contaminants increase with the decreasing particle size (Fig. 3 and Table S8†), but for the whole dataset, statistically significant differences in the total concentrations were only observed for Pb (original *versus* the <10 µm fraction) (Fig. S5†). Especially Zn in the N tailings represents an exception from this rule exhibiting lower total concentrations in the <10 µm fraction; this observation seems related to the predominantly larger fragments of the metal-bearing sulfides (10–50 µm in size) (Fig. 2e, f and S6†).

### 3.2 Metal(loid) bioaccessibility and mineralogical changes during extraction in SGF

With a few exceptions, the bioaccessible concentrations increase with the decreasing particle size of the tailings dust

(Fig. 3 and Table S8†). The bioaccessible fractions vary substantially between the sites; whereas the calculated mean BAF values for the main contaminants (Cu, Pb, Zn) for the K tailings accounted for 82 ± 17% of the total concentration, the O tailings and N tailings from the drier areas exhibited lower BAFs with values of 73 ± 20% and 22 ± 17%, respectively (Fig. 3). The differences in the BAF values for the individual metals between the K and O sites were not statistically significant, but the tailings from the hyperarid N site exhibited significantly lower BAFs than those of the other study sites (Fig. 4). The contaminant bioaccessibility is directly linked to their binding in solid phase, specific mineralogical associations, and solubility of the individual mineral constituents of the tailings. It was not possible to measure the carbonate ions in the obtained SGF extracts by standard analytical methods and to calculate the saturation state of the individual extracts with respect to the carbonates using PHREEQC-3, but, based on our previous findings,<sup>14,15</sup> we expect that the carbonates (calcite, dolomite, malachite) are prone to dissolution during the bioaccessibility testing. A comparison of XRD patterns of the carbonate-rich K tailings before and after the extraction in the SGF (Fig. S6†) confirms this hypothesis, showing that the carbonates have entirely disappeared from the dust samples. No change in the mineralogical composition during the extraction in the SGF was observed for the O samples, which are predominantly composed of stable silicate gangue minerals (Fig. S6†). The PHREEQC-3 geochemical calculations confirm that sulfides, which were identified as major metal-bearing phases in the primary tailing dust, exhibit negative SI values for all the extracts, indicating that all of them tend to be dissolved during the interaction with the highly acidic SGF (pyrite: −118 to −150; chalcocite: −131 to −167; sphalerite: −70 to −87). However, the XRD data on the <48 µm fraction of the N1 sample (Fig. S6†) confirm that this sulfide remains relatively stable during the SGF extraction, probably due to the slow

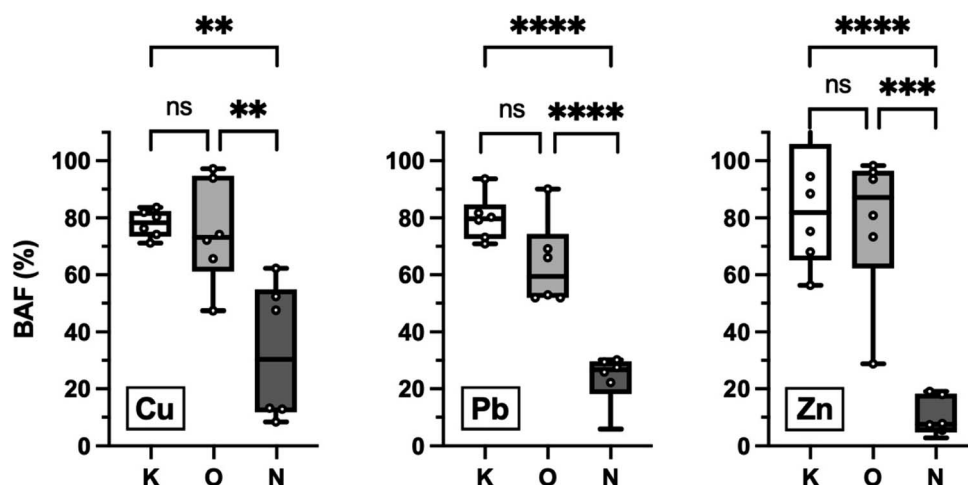


Fig. 4 Comparison of the bioaccessible fractions (BAFs, in %) of Cu, Pb, and Zn between the individual sites. Calculations using Tukey's multiple comparison test ( $\alpha = 0.05$ ) consider the whole dataset of the samples for each site (data points correspond to mean values for duplicated analyses) and indicate whether the differences are statistically significant. Asterisks correspond to the calculated *P*-values and their classification: \*  $\leq 0.05$ ; \*\*  $\leq 0.01$ ; \*\*\*  $\leq 0.001$ ; \*\*\*\*  $\leq 0.0001$ ; ns – not significant. Symbols for the individual sites: K = Kombat, O = Oamites, N = Namib Lead & Zinc.





kinetics of the sulfide dissolution or formation of alteration rims composed of Fe (oxyhydr)oxides preventing the sulfide grain dissolution (Fig. 2e). Also, despite the negative SI values calculated for gypsum, Fe (oxyhydr)oxides and Fe hydroxysulfates (e.g., gypsum:  $-4.9$  to  $-1.0$ ; goethite:  $-3.2$  to  $-1.6$ ; hematite:  $-0.9$  to  $-3.9$ ; jarosite:  $-6.0$  to  $-13.9$ ), only gypsum was dissolved entirely (Fig. S6†). In contrast, goethite, lepidocrocite, and jarosite, important metal(loid)-bearing minerals in the N tailings, are still observed in the residue after the extraction in the SGF (Fig. S6†).

### 3.3 Exposure estimates

Comparisons of the calculated daily intakes of contaminants assuming dust intakes of 100 and 280 mg per day with risk levels are reported in Table S9†. The results for major contaminants (Cu, Pb, Zn) are also depicted in Fig. 5, and the results for minor contaminants (As, Cd) are depicted in Fig. S7†. Whereas Zn intakes are far below the limits for children and adults under both exposure scenarios, Cu and Pb are more problematic contaminants. When a dust intake of 280 mg per day is assumed, most of the K and O tailings exceed the Cu minimal risk limits when children are considered targets ( $1.2$ – $17\times$ ) (Fig. 5 and Table S9†). For several samples (all particle-size fractions of K1 and sample O2  $<10\ \mu\text{m}$ ), the calculated intakes are also  $1.1$ – $2.4\times$  higher than the limit values for adults (Fig. 5 and Table S9†). At the higher modeled dust intake, practically all the samples exceed the TDI values for Pb calculated for children (up to  $55\times$ ), and this metal also becomes problematic for adults in the case of selected samples (all fractions of the K1 sample and the  $<10\ \mu\text{m}$  fractions of samples K2, O1, N1, and N2; exceedance up to  $7.9\times$ ) (Fig. 5 and Table S9†). At the dust intake of 280 mg per day, the As intakes exceeded the ATSDR minimal risk levels for chronic exposure for children in the case of K samples ( $1$ – $9.8\times$ ). Cadmium is considered critical for children in the case of K1, O1  $<10\ \mu\text{m}$ , and the selected N samples, but not for adults (Table S9 and Fig. S7†). Note that at the ingestion of 100 mg of dust per day, the Pb intake especially exceeded the TDI values for children in most samples, and As, Cd, and Cu also exceeded the limits in the case of the K1 samples (Fig. 5, S7 and Table S9†).

## 4. Discussion

### 4.1 Contaminant solid-phase partitioning in tailings from different climatic settings

The tailings from the studied sites contain elevated residual concentrations of metals and metalloids (generally up to tens of thousands  $\text{mg kg}^{-1}$ ) which agree well with similar materials reported for the tailings storage facilities from mining areas in Namibia<sup>5,14,30,32,42,43,67,68</sup> and worldwide.<sup>13,18,69–72</sup>

Contaminant binding in mine tailings might be very complex; gangue minerals (mostly carbonates and silicates) are associated with sulfides and a large variety of secondary weathering products, which include efflorescence salts, oxides and hydroxides, sulfates and hydroxysulfates, and secondary carbonates.<sup>71</sup> The studied Namibian tailings differ in the mineralogical compositions, which seem to reflect not only primary compositions of the extracted ore, but also climatic conditions. For instance, except for rare grains of chalcopryrite, sulfides are virtually missing in the tailings in a semiarid area of Kombat, the primary sulfides weathered to secondary carbonates (malachite, cerussite-like minerals) and Fe (oxyhydr)oxides (Fig. 2). Although they are also sometimes altered, intact sulfide grains are more frequently observed in the tailings from Oamites (Fig. 2d) and Namib Lead & Zinc (Fig. 2e and f). The mineralogy of the tailings is a key driver affecting the release of metal(loid)s and reflects the climate. In humid climates, soluble minerals (salts) may not accumulate due to the high precipitation rate and subsequent leaching; in contrast, in semiarid and hyperarid climates, due to the lack of water and high evaporation, the primary metal(loid)-bearing sulfides react at slower rates and newly formed soluble minerals persist.<sup>69</sup> Our data show that under the hyperarid conditions in the Namib Lead & Zinc tailings, pyrrhotite exhibits thick weathering rims composed of Fe (oxyhydr)oxides. In contrast, sphalerite and pyrite seem relatively persistent to alteration (Fig. 2e and f). This is in agreement with Moncur *et al.*<sup>73</sup> who, according to microscopic observations, established a relative order of sulfide resistance in oxidized tailings; whereas pyrite and chalcopryrite are assumed to be relatively resistant, pyrrhotite and sphalerite tend to be substantially more weathered. The formation of

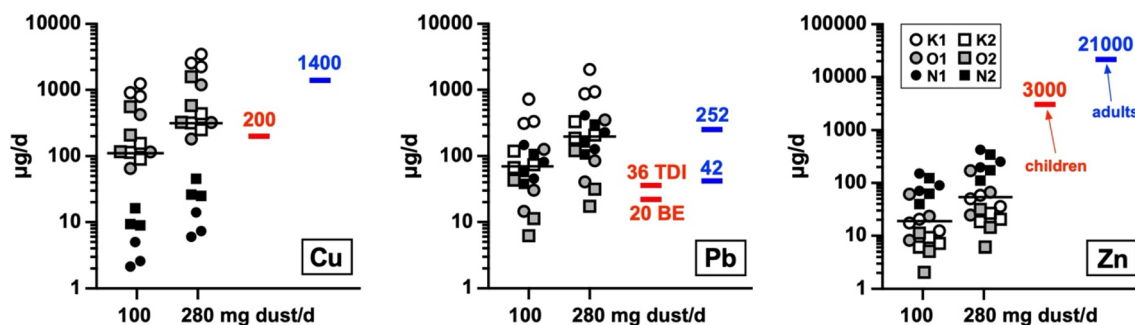


Fig. 5 Exposure estimates calculated as daily intakes of major contaminants, Cu, Pb, and Zn (in  $\mu\text{g}$  per day) assuming a dust intake of 100 mg per day and 280 mg per day and a comparison with the background exposure (BE), tolerable daily intake (TDI) limits (for Pb), and ATSDR minimal risk levels, respectively, (other contaminants) as calculated for a 10 kg child (in red) and a 70 kg adult (in blue). Black lines indicate the median value for the entire dataset. Symbols for the individual sites: K = Kombat, O = Oamites, N = Namib Lead & Zinc.



jarosite group phases and Fe (oxyhydr)oxides in an arid environment leads to the efficient sequestration of contaminants (As, Pb, Zn), especially in the surficial layers of the tailings impoundments;<sup>38,69,74</sup> this process probably also plays a key role in the stabilization of the Namib Lead & Zinc tailings.

#### 4.2 Controls on contaminant bioaccessibility

Apart from the particle size and morphology of the contaminant-bearing particles, the mineralogical composition controls the dissolution of contaminants in body fluids.<sup>75–77</sup> Our results indicate that samples with higher amounts of sulfides (e.g., Namib Lead & Zinc tailings) exhibit lower contaminant bioaccessibilities. Sulfides are generally considered the most stable during dissolution in the SGF.<sup>75</sup> This assumption has been experimentally confirmed on pure Pb minerals, indicating that galena (PbS) was the least soluble under gastric conditions.<sup>78</sup> Similarly, Molina *et al.*<sup>79</sup> showed that sphalerite (ZnS) was sparingly soluble in the SGF with BAF values accounting for only  $1.7 \pm 0.4\%$ , which agrees well with our data for the Namib Lead & Zinc tailings showing the sphalerite persistence during the oral bioaccessibility testing (Fig. S6†). Our mineralogical investigations confirmed that metal(loid) contaminants are incorporated into Fe hydroxysulfates (jarosite) and Fe (oxyhydr)oxides, especially in the tailings from arid environments (Table S7†). Despite the PHREEQC-3 calculations predicting the dissolution of these phases, the XRD data showed no evidence of their dissolution under gastric conditions (Fig. S6†), efficiently controlling the contaminant bioaccessibility. This agrees well with previous investigations showing that sequestration of As and Pb in Fe (oxyhydr)oxides and jarosite decreases their bioaccessibility.<sup>38,39</sup> Also, although equilibrium models tend to predict the dissolution of Fe (oxyhydr)oxides under gastric conditions (pH about 1.5), experimental studies document their stability, probably due to kinetic reasons.<sup>15,80,81</sup> Further weathering of Pb-jarosite and Pb-bearing Fe (oxyhydr)oxides to anglesite (PbSO<sub>4</sub>) in the surface layers of tailings weathered under (semi)arid conditions would increase the Pb bioaccessibility.<sup>37</sup> However, this process has not been documented at any of the studied Namibian sites.

Substantially higher bioaccessibilities are often related to more soluble phases, such as carbonates, which dissolve under gastric conditions.<sup>14,15,18,26,28</sup> This situation mainly occurs in the Kombat tailings, where metal carbonates were identified as the major contaminant hosts (Table S7†) where the BAF fractions attain 100%.

#### 4.3 Environmental implications and recommendations to minimize exposure

Our results indicate that, compared to the other two study sites, Kombat is the most problematic locality for potential human health impacts due to (i) the vicinity of the settlement (Fig. S2a†), (ii) the highest bioaccessibility of contaminants related to their occurrence in minerals, which are very soluble in gastric environments (Fig. 2–5), and (iii) a substantially higher percentage of wind-erodible particles (Table S1†). Moreover, at Kombat the surface of tailings is visually less compacted and

prone to dust generation compared to e.g., Namib Lead & Zinc site (Fig. 1). Wind plays a key role in the aeolian erosion and subsequent dispersion of tailing particles in semiarid and arid systems.<sup>3,10</sup> Ojelede *et al.*<sup>82</sup> reported that at wind speeds exceeding  $7 \text{ m s}^{-1}$ , PM<sub>10</sub> (particulate matter < 10 µm) concentrations reached  $2160 \text{ µg m}^{-3}$  near gold mine tailings under (semi)arid conditions in South Africa. In the past, *Prosopis* sp. trees and bushes were planted on the surface of the Kombat tailings storage facility to phytostabilize it and limit the dust dispersion; however, this stabilization effort was not very successful.<sup>5</sup> Other remediation options include capping<sup>18,83</sup> or watering the surface of the tailings impoundment, although a sufficient supply of water is always problematic in semiarid or arid areas. Based on the monitoring results obtained by low-volume portable samplers, Křibek *et al.*<sup>84</sup> modeled dust emissions from tailings storage facilities in arid southern Namibia and found that suspended dust particles markedly decreased from 100–300 to 30–100 µg m<sup>−3</sup> when two-thirds of the tailings dam surface has been covered with water. The recent re-opening of the mining operations in Kombat represents a unique opportunity to improve the management of the existing tailings storage facilities (remediation, potential reprocessing) and to construct new tailings dams in an environment-friendly way (e.g., reusing the water pumped from the underground mine for watering the surface of the tailings impoundment). Moreover, additional multifaceted investigations should be carried out in the future to evaluate the risk for human health better (e.g., by analyzing the soil and household dust samples combined with a biomarker-exposure approach<sup>19,23,85</sup>) as well as for the farmland animals and crops.

## 5. Conclusions

Fine dust fractions from tailings storage facilities of abandoned metal mines in Kombat, Oamites, and Namib Lead & Zinc (Namibia), situated along a climatic gradient from semiarid to desert environments, were investigated. A multi-method geochemical and mineralogical characterization was combined with oral bioaccessibility testing on <48 µm and <10 µm particle-size fractions followed by human health risk assessment calculations. The bioaccessible fractions of inorganic contaminants (with emphasis on Cu, Pb, and Zn being the most abundant metals) decreased as a function of the increasing aridity. The lowest contaminant bioaccessibilities were observed in the tailings from the Namib Lead & Zinc mine, situated in an arid environment, where metal(loid) contaminants were primarily bound in sulfides, Fe (oxyhydr)oxides, and Fe hydroxysulfates insoluble in the simulated gastric fluid. In contrast, the tailings from Kombat, where the annual precipitation attains ~500 mm, were highly weathered and composed of metal-hosting carbonates, which entirely dissolved under gastric conditions. Thus, compared to the other two more arid sites with much lower or zero precipitation, the Kombat tailings dam represents the highest risk for the local population due to nearby settlements and farmlands used for crop and animal production. The recent re-opening of mining activities in the area provides a unique opportunity to improve the management



of the tailings in an environment-friendly way and to minimize human health and ecosystem impacts.

## Data availability

The data for this article have been included as part of the ESI† and are also available at Zenodo at <https://doi.org/10.5281/zenodo.14731259>.

## Author contributions

Vojtěch Ettler: conceptualization, data curation, formal analysis, funding acquisition, investigation, methodology, project administration, resources, supervision, validation, visualization, roles/writing – original draft, writing – review & editing. Tereza Křížová: data curation, formal analysis, investigation, methodology, resources, writing – review & editing. Martin Mihaljevič: data curation, formal analysis, funding acquisition, investigation, project administration, resources, writing – review & editing. Petr Drahota: data curation, formal analysis, investigation, resources, writing – review & editing. Martin Racek: investigation, data curation, formal analysis, resources. Bohdan Kříbek: data curation, investigation, project administration, resources, writing – review & editing. Aleš Vaněk: investigation, resources, writing – review & editing. Vít Penížek: investigation, resources. Ondra Sracek: investigation, resources, writing – review & editing. Ban Mapani: investigation, project administration, resources, writing – review & editing.

## Conflicts of interest

The authors declare that they have no known competing financial interests or personal relationships that could have appeared to influence the work reported in this paper.

## Acknowledgements

This study was supported by the Czech Science Foundation (GAČR project 23-05051S) and the Johannes Amos Comenius Programme (P JAC), project No. CZ.02.01.01/00/22\_008/0004605, Natural and anthropogenic georisks. We thank many colleagues for their help in the laboratory (Marie Fayadová, Věra Vonásková, Lenka Jílková). We also greatly acknowledge the Namib Lead & Zinc Mine management, especially Daan van Staden, plant manager of the Namib Lead & Zinc Mining company, for his assistance and help during the field sampling. Alan Harvey Cook is also thanked for revising the English in this manuscript. The thorough reviews of two anonymous referees helped to substantially improve the paper.

## References

- 1 J. Csavina, J. Field, M. P. Taylor, S. Gao, A. Landázuri, E. A. Betterton and A. E. Sáez, A review on the importance of metals and metalloids in atmospheric dust and aerosol from mining operations, *Sci. Total Environ.*, 2012, **433**, 58–73, DOI: [10.1016/j.scitotenv.2012.06.013](https://doi.org/10.1016/j.scitotenv.2012.06.013).
- 2 J. Kasongo, L. Y. Alleman, J. M. Kanda, A. Kaniki and V. Riffault, Metal-bearing airborne particles from mining activities: a review on their characteristics, impacts and research perspectives, *Sci. Total Environ.*, 2024, **951**, 175426, DOI: [10.1016/j.scitotenv.2024.175426](https://doi.org/10.1016/j.scitotenv.2024.175426).
- 3 N. C. Zanetta-Colombo, C. A. Manzano, D. Brombierstäudl, Z. L. Fleming, E. M. Gayo, D. A. Rubinos, Ó. Jerez, J. Valdés, M. Prieto and M. Nüsser, Blowin' in the wind: mapping the dispersion of metal(loid)s from Atacam mining, *GeoHealth*, 2024, **8**, e2024GH001078, DOI: [10.1029/2024GH001078](https://doi.org/10.1029/2024GH001078).
- 4 B. Mapani, R. Ellmies, F. Kamona, B. Kříbek, V. Majer, I. Knésl, J. Pašava, M. Mufenda and F. Mbingeneeko, Potential human health risks associated with historic ore processing at Berg Aukas, Grootfontein area, Namibia, *J. Afr. Earth Sci.*, 2010, **58**, 634–647, DOI: [10.1016/j.afrearsci.2010.07.007](https://doi.org/10.1016/j.afrearsci.2010.07.007).
- 5 M. Mileusnić, B. S. Mapani, A. F. Kamona, S. Ružičić, I. Mapaure and P. M. Chimwamurombe, Assessment of agricultural soil contamination by potentially toxic metals dispersed from improperly disposed tailings, Kombat mine, Namibia, *J. Geochem. Explor.*, 2014, **144**, 409–420, DOI: [10.1016/j.gexplo.2014.01.009](https://doi.org/10.1016/j.gexplo.2014.01.009).
- 6 B. Kříbek, V. Majer, I. Knésl, I. Nyambe, M. Mihaljevič, V. Ettler and O. Sracek, Concentrations of arsenic, copper, cobalt, lead and zinc in cassava (*Manihot esculenta* Crantz) growing on uncontaminated and contaminated soils of the Zambian Copperbelt, *J. Afr. Earth Sci.*, 2014, **99**, 713–723, DOI: [10.1016/j.efrenvsci.2014.02.009](https://doi.org/10.1016/j.efrenvsci.2014.02.009).
- 7 V. Ettler, Soil contamination near non-ferrous metal smelters: a review, *Appl. Geochem.*, 2016, **64**, 56–74, DOI: [10.1016/j.apgeochem.2015.09.020](https://doi.org/10.1016/j.apgeochem.2015.09.020).
- 8 A. Parviainen, A. Vázquez-Arias and F. J. Martín-Peinado, Mineralogical association and geochemistry of potentially toxic elements in urban soils under the influence of mining, *Catena*, 2022, **217**, 106517, DOI: [10.1016/j.catena.2022.106517](https://doi.org/10.1016/j.catena.2022.106517).
- 9 A. Parviainen, A. Vázquez-Arias, J. P. Arrebola and F. J. Martín-Peinado, Human health risks associated with urban soils in mining areas, *Environ. Res.*, 2022, **206**, 112514, DOI: [10.1016/j.envres.2021.112514](https://doi.org/10.1016/j.envres.2021.112514).
- 10 P. I. Beamer, A. J. Sugeng, M. D. Kelly, N. Lothrop, W. Klimecki, S. T. Wilkinson and M. Loh, Use of dust fall filters as passive samplers for metal concentrations in air for communities near contaminated mine tailings, *Environ. Sci.: Processes Impacts*, 2014, **16**, 1275–1281, DOI: [10.1039/c3em00626c](https://doi.org/10.1039/c3em00626c).
- 11 J. A. Entwistle, A. S. Hursthouse, P. A. M. Reis and A. G. Stewart, Metalliferous mine dust: human health impacts and the potential determinants of disease in mining communities, *Curr. Pollut. Rep.*, 2019, **5**, 67–83, DOI: [10.1007/s40726-019-00108-5](https://doi.org/10.1007/s40726-019-00108-5).
- 12 J. Li and J. McDonald-Gillespie, Airborne lead (Pb) from abandoned mine waste in northeastern Oklahoma, USA, *GeoHealth*, 2020, **4**, e2020GH000273, DOI: [10.1029/2020GH000273](https://doi.org/10.1029/2020GH000273).





- 13 C. S. J. Eulises, M. C. A. González-Chávez, R. Carrillo-González, J. L. García-Cué, D. S. Fernández-Reynoso, M. Noerpel and K. G. Scheckel, Bioaccessibility of potentially toxic elements in mine residue particles, *Environ. Sci.:Processes Impacts*, 2021, **23**, 367, DOI: [10.1039/d0em00447b](https://doi.org/10.1039/d0em00447b).
- 14 V. Ettler, M. Cihlová, A. Jarošíková, M. Mihaljevič, P. Drahota, B. Kříbek, A. Vaněk, V. Penížek, O. Sracek, M. Klementová, Z. Engel, F. Kamona and B. Mapani, Oral bioaccessibility of metal(loid)s in dust materials from mining areas of northern Namibia, *Environ. Int.*, 2019, **124**, 205–215, DOI: [10.1016/j.envint.2018.12.027](https://doi.org/10.1016/j.envint.2018.12.027).
- 15 V. Ettler, D. Štěpánek, M. Mihaljevič, P. Drahota, R. Jedlicka, B. Kříbek, A. Vaněk, V. Penížek, O. Sracek and I. Nyambe, Slag dusts from Kabwe (Zambia): contaminant mineralogy and oral bioaccessibility, *Chemosphere*, 2020, **260**, 127642, DOI: [10.1016/j.chemosphere.2020.127642](https://doi.org/10.1016/j.chemosphere.2020.127642).
- 16 V. Ettler, K. Hladíková, M. Mihaljevič, P. Drahota, A. Culka, R. Jedlicka, B. Kříbek, A. Vaněk, V. Penížek, O. Sracek and Z. Bagai, Contaminant binding and bioaccessibility in the dust from the Ni–Cu mining/smeltering district of Selebi-Phikwe (Botswana), *GeoHealth*, 2022, **6**, e2022GH000683, DOI: [10.1029/2022GH000683](https://doi.org/10.1029/2022GH000683).
- 17 V. Ettler, K. Raus, M. Mihaljevič, B. Kříbek, A. Vaněk, V. Penížek, O. Sracek, M. Koubová and B. Mapani, Bioaccessible metals in dust materials from non-sulfide Zn deposit and related hydrometallurgical operation, *Chemosphere*, 2023, **345**, 140498, DOI: [10.1016/j.chemosphere.2023.140498](https://doi.org/10.1016/j.chemosphere.2023.140498).
- 18 J. Helser, E. Vassilieva and V. Cappuyns, Environmental and human health risk assessment of sulfidic mine waste: bioaccessibility, leaching and mineralogy, *J. Hazard. Mater.*, 2022, **424**, 127313, DOI: [10.1016/j.hazmat.2021.127313](https://doi.org/10.1016/j.hazmat.2021.127313).
- 19 C. L. N. Banza, T. S. Nawrot, V. Haufroid, S. Decrée, T. De Putter, E. Smolders, B. I. Kabyla, O. N. Luboya, A. N. Ilunga, A. M. Mutombo and B. Nemery, High human exposure to cobalt and other metals in Katanga, a mining area of the Democratic Republic of Congo, *Sci. Total Environ.*, 2009, **109**, 745–752, DOI: [10.1016/j.scitotenv.2009.04.012](https://doi.org/10.1016/j.scitotenv.2009.04.012).
- 20 K. Cheyns, C. B. L. Nkulu, L. K. Ngombe, J. N. Asosa, V. Haufroid, T. De Putter, T. Nawrot, C. M. Kimpanga, O. L. Numbi, B. K. Ilunga, B. Nemery and E. Smolders, Pathways of human exposure to cobalt in Katanga, a mining area of the D. R. Congo, *Sci. Total Environ.*, 2014, **490**, 313–321, DOI: [10.1016/j.scitotenv.2014.05.014](https://doi.org/10.1016/j.scitotenv.2014.05.014).
- 21 E. Smolders, L. Roels, T. C. Kuhangana, K. Coorevits, E. Vassilieva, B. Nemery and C. B. L. Nkulu, Unprecedentedly high dust ingestion estimates for the general population in a mining district of DR Congo, *Environ. Sci. Technol.*, 2019, **53**, 7851–7858, DOI: [10.1021/acs.est.9b01973](https://doi.org/10.1021/acs.est.9b01973).
- 22 A. R. Mwesigye, S. D. Young, E. H. Bailey and S. B. Tumwebaze, Population exposure to trace elements in the Kilembe copper mine area, Western Uganda: a pilot study, *Sci. Total Environ.*, 2016, **573**, 366–375, DOI: [10.1016/j.scitotenv.2016.08.125](https://doi.org/10.1016/j.scitotenv.2016.08.125).
- 23 J. Yabe, S. M. M. Nakayama, H. Nakata, H. Toyomaki, Y. B. Yohannes, K. Muzandu, A. Kataba, G. Zyambo, M. Hiwatari, D. Narita, D. Yamada, P. Hangoma, N. S. Munyinda, T. Mufune, Y. Ikenaka, K. Choongo and M. Ishizuka, Current trends in blood lead levels, distribution patterns and exposure variations among household members in Kabwe, Zambia, *Chemosphere*, 2020, **243**, 125412, DOI: [10.1016/j.chemosphere.2019.125412](https://doi.org/10.1016/j.chemosphere.2019.125412).
- 24 O. Bello, R. Naidu, M. M. Rahman, Y. Liu and Z. Dong, Lead concentration in the blood of the general population living near a lead–zinc mine site, Nigeria: exposure pathways, *Sci. Total Environ.*, 2016, **542**, 908–914, DOI: [10.1016/j.scitotenv.2015.10.143](https://doi.org/10.1016/j.scitotenv.2015.10.143).
- 25 V. Ettler, B. Kříbek, V. Majer, I. Kněsl and M. Mihaljevič, Differences in the bioaccessibility of metals/metalloids in soils from mining and smelting areas (Copperbelt, Zambia), *J. Geochem. Explor.*, 2012, **113**, 68–75, DOI: [10.1016/j.gexplo.2011.08.001](https://doi.org/10.1016/j.gexplo.2011.08.001).
- 26 M. Ghorbel, M. Munoz, P. Courjault-Radé, C. Destigneville, P. de Perseval, R. Souissi, F. Souissi, A. Ben Mammou and S. Abdeljaouad, Health risk assessment for human exposure by direct ingestion of Pb, Cd, Zn bearing dust in the former miners' village of Jebel Ressa (NE Tunisia), *Eur. J. Mineral.*, 2010, **22**, 639–649, DOI: [10.1127/0935-1221/2010/0022-2037](https://doi.org/10.1127/0935-1221/2010/0022-2037).
- 27 V. Ettler, M. Vítková, M. Mihaljevič, O. Šebek, M. Klementová, F. Veselovský, P. Vybiral and B. Kříbek, Dust from Zambian smelters: mineralogy and contaminant bioaccessibility, *Environ. Geochem. Health*, 2014, **36**, 919–933, DOI: [10.1007/s10653-014-9609-4](https://doi.org/10.1007/s10653-014-9609-4).
- 28 L. Nejeschlebová, O. Sracek, M. Mihaljevič, V. Ettler, B. Kříbek, I. Kněsl, A. Vaněk, V. Penížek, Z. Dolníček and B. Mapani, Geochemistry and potential environmental impact of the mine tailings at Rosh Pinah, southern Namibia, *J. Afr. Earth Sci.*, 2015, **105**, 17–28, DOI: [10.1016/j.afrearsci.2015.02.005](https://doi.org/10.1016/j.afrearsci.2015.02.005).
- 29 A. T. Salom and S. Kivinen, Closed and abandoned mines in Namibia: a critical review of environmental impacts and constraints to rehabilitation, *S. Afr. Geogr. J.*, 2020, **102**, 389–405, DOI: [10.1080/03736245.2019.1698450](https://doi.org/10.1080/03736245.2019.1698450).
- 30 L. Hahn, F. Solesbury and S. Mwiya, Report: assessment of potential environmental impacts and rehabilitation of abandoned mine sites in Namibia, *Comm. Geol. Survey Namibia*, 2004, **13**, 85–91.
- 31 I. Hasheela, G. I. C. Schneider, R. Ellmies, A. Haidula, R. Leonard, K. Ndalulilwa, O. Shigwana and B. Walmsley, Risk assessment methodology for shut-down and abandoned mine sites in Namibia, *J. Geochem. Explor.*, 2014, **144**, 572–580, DOI: [10.1016/j.gexplo.2014.05.009](https://doi.org/10.1016/j.gexplo.2014.05.009).
- 32 M. N. Uugwanga and N. A. Kgabi, Assessment of metals pollution in sediments and tailings of Klein Aub and Oamites mine sites, Namibia, *Environ. Adv.*, 2020, **2**, 100006, DOI: [10.1016/j.envadv.2020.100006](https://doi.org/10.1016/j.envadv.2020.100006).



- 33 M. N. Ugwanga and N. A. Kgabi, Dilution and dispersion of particulate matter from abandoned mine sites to nearby communities in Namibia, *Heliyon*, 2021, 7, e06643, DOI: [10.1016/j.heliyon.2021.e06643](https://doi.org/10.1016/j.heliyon.2021.e06643).
- 34 P. Drahota, V. Ettler, A. Culka, J. Rohovec and R. Jedlička, Effect of relative humidity on oxidation products of arsenopyrite and löllingite, *Chem. Geol.*, 2022, **605**, 120945, DOI: [10.1016/j.chemgeo.2022.120945](https://doi.org/10.1016/j.chemgeo.2022.120945).
- 35 J. Gerding, A. A. Novoselov and J. Morales, Climate and pyrite: Two factors to control the evolution of abandoned tailings in Northern Chile, *J. Geochem. Explor.*, 2021, **221**, 106686, DOI: [10.1016/j.gexplo.2020.106686](https://doi.org/10.1016/j.gexplo.2020.106686).
- 36 L. Haffert, D. Craw and J. Pope, Climatic and compositional controls on secondary arsenic mineral formation in high-arsenic mine wastes, South Island, New Zealand, *N. Z. J. Geol. Geophys.*, 2010, **53**, 91–101, DOI: [10.1080/00288306.2010.498403](https://doi.org/10.1080/00288306.2010.498403).
- 37 S. M. Hayes, S. M. Webb, J. R. Bargar, P. A. O'Day, R. M. Maier and J. Chorover, Geochemical weathering increases lead bioaccessibility in semi-arid mine tailings, *Environ. Sci. Technol.*, 2012, **46**, 5834–5841, DOI: [10.1021/es300603s](https://doi.org/10.1021/es300603s).
- 38 A. N. Thomas, R. A. Root, R. C. Lantz, E. Sáez and J. Chorover, Oxidative weathering decreases bioaccessibility of toxic metal(loid)s in PM10 emission from sulfide mine tailings, *GeoHealth*, 2018, **2**, 118–138, DOI: [10.1002/2017GH000118](https://doi.org/10.1002/2017GH000118).
- 39 R. A. Root and J. Chorover, Molecular speciation controls arsenic and lead bioaccessibility in fugitive dusts from sulfidic mine tailings, *Environ. Sci.: Processes Impacts*, 2023, **25**, 288–303, DOI: [10.1039/d2em00182a](https://doi.org/10.1039/d2em00182a).
- 40 R. Shikangalah, A. Musimba, I. Mapaure, B. Mapani, U. Herzsuh, X. Tabares and C. Kamburona-Ngavetene, Growth rings and stem diameter of *Dichrostachys cinerea* and *Senegalia mellifera* along a rainfall gradient in Namibia, *Trees Forest People*, 2021, **3**, 100046, DOI: [10.1016/j.tfp.2020.100046](https://doi.org/10.1016/j.tfp.2020.100046).
- 41 L. Naftal, V. De Cauwer and B. J. Strohbach, Potential distribution of major plant units under climate change scenarios along an aridity gradient in Namibia, *Veg. Classif. Surv.*, 2024, **5**, 127–151, DOI: [10.3897/VCS.99050](https://doi.org/10.3897/VCS.99050).
- 42 O. Sracek, M. Mihaljevič, B. Kříbek, V. Majer, J. Filip, A. Vaněk, V. Penížek, V. Ettler and B. Mapani, Geochemistry of mine tailings and behavior of arsenic at Kombat, northeastern Namibia, *Environ. Monit. Assess.*, 2014, **186**, 4891–4903, DOI: [10.1007/s10661-014-3746-1](https://doi.org/10.1007/s10661-014-3746-1).
- 43 M. Mihaljevič, R. Baieta, V. Ettler, A. Vaněk, B. Kříbek, V. Penížek, P. Drahota, J. Trubač, O. Sracek, V. Chrástný and B. S. Mapani, Tracing the metal dynamics in semi-arid soils near mine tailings using stable Cu and Pb isotopes, *Chem. Geol.*, 2019, **515**, 61–76, DOI: [10.1016/j.chemgeo.2019.03.026](https://doi.org/10.1016/j.chemgeo.2019.03.026).
- 44 M. Kottek, J. Griesen, C. Beck, B. Rudolf and F. Rubel, World Map of the Köppen–Geiger climate classification updated, *Meteorol. Z.*, 2006, **15**, 259–263, DOI: [10.1127/0941-2948/2006/0130](https://doi.org/10.1127/0941-2948/2006/0130).
- 45 World Bank, *Climate Change Knowledge Portal. Namibia*, <https://climateknowledgeportal.worldbank.org/country/namibia>, date accessed: 18 October 2024.
- 46 O. Sracek, V. Ettler, B. Kříbek, M. Mihaljevič, B. Mapani, V. Penížek, T. Zádorová and A. Vaněk, Characterization and stable isotopic fingerprinting of mine seepage in hyperarid environments: an example of the Namib Lead & Zinc mine, Namibia, *J. Geochem. Explor.*, 2024, **265**, 107554, DOI: [10.1016/j.gexplo.2024.107554](https://doi.org/10.1016/j.gexplo.2024.107554).
- 47 GEMAS, *EuroGeoSurveys Geochemical Mapping of Agricultural and Grazing Land Soil of Europe (GEMAS) – Field Manual. Report 2008.038*. Geological Survey of Norway, Trondheim, 2008, p. 46.
- 48 S. D. Siciliano, K. James, G. Zhang, A. N. Schafer and J. D. Peak, Adhesion and enrichment of metals on human hands from contaminated soil at an arctic urban brownfield, *Environ. Sci. Technol.*, 2009, **43**, 6385–6390, DOI: [10.1021/es901090w](https://doi.org/10.1021/es901090w).
- 49 J. R. H. Smith, G. Etherington, A. L. Shutt and M. J. Youngman, A study of aerosol deposition and clearance from the human nasal passage, *Ann. Occup. Hyg.*, 2002, **46**(Suppl. 1), 309–313, DOI: [10.1093/annhyg/46.suppl\\_1.309](https://doi.org/10.1093/annhyg/46.suppl_1.309).
- 50 T. C. Carvalho, J. I. Peters and R. O. Williams III, Influence of particle size on regional lung deposition – what evidence is there, *Int. J. Pharm.*, 2011, **406**, 1–10, DOI: [10.1016/j.ijpharm.2010.12.040](https://doi.org/10.1016/j.ijpharm.2010.12.040).
- 51 ISO 10390, *Soil, Treated Biowaste and Sludge – Determination of pH*, ISO, Geneva, 2021.
- 52 S. Gražulis, A. Daškevič, A. Merkys, D. Chateigner, L. Lutterotti, M. Quirós, N. R. Serebryanaya, P. Moeck, R. T. Downs and A. Le Bail, Crystallography Open Database (COD): an open-access collection of crystal structures and platform for worldwide collaboration, *Nucleic Acids Res.*, 2012, **40**, D420–D427, DOI: [10.1093/nar/gkr900](https://doi.org/10.1093/nar/gkr900).
- 53 US EPA, *SW-846 Test Method 1340, In Vitro Bioaccessibility Assay for Lead in Soil*, US EPA, Washington, 2017, <https://www.epa.gov/hw-sw846/sw-846-test-method-1340-vitro-bioaccessibility-assay-lead-soil>.
- 54 M. Dodd, D. Lee, J. Nelson, S. Verenitch and R. Wilson, *In vitro* bioaccessibility round robin testing for arsenic and lead in standard reference materials and soil samples, *Integr. Environ. Assess. Manage.*, 2024, **20**, 1486–1495, DOI: [10.1002/ieam.4891](https://doi.org/10.1002/ieam.4891).
- 55 J. Bierkens, M. Van Holderbeke, C. Cornelis and R. Torfs, Exposure Through Soil and Dust Ingestion, in *Dealing with Contaminated Sites*, ed. Swartjes, F. A., Springer Science + Business Media B.V., Berlin, 2011, pp. 261–286.
- 56 ATSDR, *Minimal Risk Levels (MRLs)*, Agency for Toxic Substances and Disease Registry, Atlanta, USA, 2024. <https://www.atsdr.cdc.gov/minimal-risk-levels/about/index.html>.
- 57 A. J. Baars, R. M. C. Theelen, P. J. C. M. Janssen, J. M. Hesse, M. E. van Apeldoorn, M. C. M. Meijerink, L. Verdam and M. J. Zeilmaker, *Re-Evaluation of Human-Toxicological Maximum Permissible Risk Levels*, RIVM Report 711701025, Bilthoven, the Netherlands, 2021.
- 58 B. Tiesjema and A. J. Baars, *Re-evaluation of Some Human-Toxicological Maximum Permissible Risk Levels Earlier*



- Evaluated in the Period 1991–2001, RIVM Report 711701092*, Bilthoven, the Netherlands, 2009.
- 59 EFSA, Cadmium in food. Scientific opinion of the Panel on Contaminants in the Food Chain, *EFSA J.*, 2009, **980**, 1–139, DOI: [10.2903/j.efsa.2009.980](https://doi.org/10.2903/j.efsa.2009.980).
  - 60 EFSA, Scientific Opinion on the risks to public health related to the presence of nickel in food and drinking water, *EFSA J.*, 2015, **13**, 4002, DOI: [10.2903/j.efsa.2015.4002](https://doi.org/10.2903/j.efsa.2015.4002).
  - 61 EFSA, Scientific opinion on lead in food, *EFSA J.*, 2010, **8**, 1570, DOI: [10.2903/j.efsa.2010.1570](https://doi.org/10.2903/j.efsa.2010.1570).
  - 62 EFSA, Dietary exposure to inorganic arsenic in the European population, *EFSA J.*, 2014, **12**, 3597, DOI: [10.2903/j.efsa.2014.3597](https://doi.org/10.2903/j.efsa.2014.3597).
  - 63 US EPA, *Regional Screening Levels (RSLs) – Generic Tables*, US EPA, Washington, 2024, <https://www.epa.gov/risk/regional-screening-levels-rsls-generic-tables>.
  - 64 D. L. Parkhurst and C. A. J. Appelo, Description of input and examples for PHREEQC version 3–A computer program for speciation, batch-reaction, one-dimensional transport, and inverse geochemical calculations, *US Geological Survey Techniques and Methods*, book 6, chap. A43, 2013.
  - 65 L. N. Warr, IMA-CNMNC approved mineral symbols, *Mineral. Mag.*, 2021, **85**, 291–320, DOI: [10.1180/mgm.2021.43](https://doi.org/10.1180/mgm.2021.43).
  - 66 J. E. Lee and D. A. Glenister, Stratiform sulfide mineralization at Oamites copper mine, South West Africa, *Econ. Geol.*, 1976, **71**, 369–383, DOI: [10.2113/gsecongeo.71.1.369](https://doi.org/10.2113/gsecongeo.71.1.369).
  - 67 S. Lohmeier, D. Gallhofer and B. G. Lottermoser, Field-portable X-ray fluorescence analyzer for chemical characterization of carbonate-bearing base metal tailings: case study from Namib Pb–Zn Mine, Namibia, *J. South. Afr. Inst. Min. Metall.*, 2024, **124**, 421–436, DOI: [10.17159/2411-9717/2676/2024](https://doi.org/10.17159/2411-9717/2676/2024).
  - 68 S. Lohmeier, D. Gallhofer and B. G. Lottermoser, Geochemical and mineralogical characterization and resource potential of the Namib Pb–Zn tailings (Erongo Region, Namibia), *J. South. Afr. Inst. Min. Metall.*, 2024, **124**, 447–459, DOI: [10.17159/2411-9717/2724/2024](https://doi.org/10.17159/2411-9717/2724/2024).
  - 69 S. M. Hayes, S. A. White, T. L. Thompson, R. M. Maier and J. Chorover, Changes in lead and zinc lability during weathering-induced acidification of desert mine tailings: coupling chemical and micro-scale analyses, *Appl. Geochem.*, 2009, **24**, 2234–2245, DOI: [10.1016/j.apgeochem.2009.09.010](https://doi.org/10.1016/j.apgeochem.2009.09.010).
  - 70 D. Kossoff, W. E. Dubbin, M. Alfredsson, S. J. Edwards, M. G. Macklin and K. A. Hudson-Edwards, Mine tailings dams: Characteristics, failure, environmental impacts, and remediation, *Appl. Geochem.*, 2014, **51**, 229–245, DOI: [10.1016/j.apgeochem.2014.09.010](https://doi.org/10.1016/j.apgeochem.2014.09.010).
  - 71 M. B. J. Lindsay, M. C. Moncur, J. G. Bain, J. L. Jambor, C. J. Ptacek and D. W. Blowes, Geochemical and mineralogical aspects of sulfide mine tailings, *Appl. Geochem.*, 2015, **57**, 157–177, DOI: [10.1016/j.apgeochem.2015.01.009](https://doi.org/10.1016/j.apgeochem.2015.01.009).
  - 72 D. A. Rubinos, Ó. Jerez, G. Forghani, M. Edraki and U. Kelm, Geochemical stability of potentially toxic elements in porphyry copper-mine tailings from Chile as linked to ecological and human health risks assessment, *Environ. Sci. Pollut. Res.*, 2021, **28**, 57499–57529, DOI: [10.1007/s11356-021-12844-7](https://doi.org/10.1007/s11356-021-12844-7).
  - 73 M. C. Moncur, J. L. Jambor, C. J. Ptacek and D. W. Blowes, Mine drainage from the weathering of sulfide minerals and magnetite, *Appl. Geochem.*, 2009, **24**, 2362–2373, DOI: [10.1016/j.apgeo.2009.09.013](https://doi.org/10.1016/j.apgeo.2009.09.013).
  - 74 R. A. Root, S. M. Hayes, C. M. Hammond, R. M. Maier and J. Chorover, Toxic metal(loid) speciation during weathering of iron sulfide mine tailings under semi-arid climate, *Appl. Geochem.*, 2015, **62**, 131–149, DOI: [10.1016/j.apgeochem.2015.01.005](https://doi.org/10.1016/j.apgeochem.2015.01.005).
  - 75 M. V. Ruby, R. Schoof, W. Brattin, M. Goldade, G. Post, M. Harnois, D. E. Mosby, S. W. Catseel, W. Berti, M. Carpenter, D. Edwards, D. Cragin and W. Chapell, Advances in evaluating the oral bioavailability of inorganics in soil for use in human health risk assessment, *Environ. Sci. Technol.*, 1999, **33**, 3697–3705, DOI: [10.1021/es990479z](https://doi.org/10.1021/es990479z).
  - 76 E. Hettiarachchi, S. Paul, D. Cadol, B. Frey and G. Rubasinghege, Mineralogy controlled dissolution of uranium from airborne dust in simulated lung fluids (SLFs) and possible health implications, *Environ. Sci. Technol. Lett.*, 2019, **6**, 62–67, DOI: [10.1021/acs.estlett.8b00557](https://doi.org/10.1021/acs.estlett.8b00557).
  - 77 E. Hettiarachchi, M. Das, D. Cadol, B. A. Frey and G. Rubasinghege, The fate of inhaled uranium-containing particles upon clearance to gastrointestinal tract, *Environ. Sci.:Processes Impacts*, 2022, **24**, 1257–1266, DOI: [10.1039/d2em00209d](https://doi.org/10.1039/d2em00209d).
  - 78 S. T. Bosso and J. Enzweiler, Bioaccessible lead in soils, slag, and mine wastes from an abandoned mining district in Brazil, *Environ. Geochem. Health*, 2008, **30**, 219–229, DOI: [10.1007/s10653-007-9110-4](https://doi.org/10.1007/s10653-007-9110-4).
  - 79 R. M. Molina, L. A. Schaidler, T. C. Donaghey, J. P. Shine and J. D. Brain, Mineralogy affects geoavailability, bioaccessibility and bioavailability of zinc, *Environ. Pollut.*, 2013, **182**, 217–224, DOI: [10.1016/j.envpol.2013.07.013](https://doi.org/10.1016/j.envpol.2013.07.013).
  - 80 C. Mikutta, P. N. Mandaliev, N. Mahler, T. Kotsev and R. Kretzschmar, Bioaccessibility of arsenic in mining-impacted circumneutral river floodplain soils, *Environ. Sci. Technol.*, 2014, **48**, 13468–13477, DOI: [10.1021/es502635t](https://doi.org/10.1021/es502635t).
  - 81 R. Liu, S. Kong, Y. Shao, D. Cai, B. Bau, X. Wei, R. A. Root, X. Gao, C. Li and J. Chorover, Mechanisms and health implications of toxicity increment from arsenate-containing iron minerals through *in vitro* gastrointestinal digestion, *Geoderma*, 2023, **432**, 116377, DOI: [10.1016/j.geoderma.2023.116377](https://doi.org/10.1016/j.geoderma.2023.116377).
  - 82 M. E. Ojelede, H. J. Annegarn and M. A. Kneen, Evaluation of aeolian emissions from gold mine tailings on the Witwatersrand, *Aeolian Res.*, 2012, **3**, 477–486, DOI: [10.1016/j.aeolia.2011.03.010](https://doi.org/10.1016/j.aeolia.2011.03.010).
  - 83 A. Zhang, J. G. Bain, A. Schmall, C. J. Ptacek and D. W. Blowes, Geochemistry and mineralogy of legacy tailings under a composite cover, *Appl. Geochem.*, 2023, **159**, 105819, DOI: [10.1016/j.apgeochem.2023.105819](https://doi.org/10.1016/j.apgeochem.2023.105819).





- 84 B. Křibek, V. Majer, J. Pašava, F. Kamona, B. Mapani, J. Keder and V. Ettler, Contamination of soils with dust fallout from the tailings dam at the Rosh Pinah area, Namibia: regional assessment, dust dispersion modeling and environmental consequences, *J. Geochem. Explor.*, 2014, **144**, 391–408, DOI: [10.1016/j.gexplo.2014.01.010](https://doi.org/10.1016/j.gexplo.2014.01.010).
- 85 A. P. M. Reis, M. Cave, A. J. Sousa, J. Wragg, M. J. Rangel, A. R. Oliveira, C. Patinha, F. Rocha, T. Orsiere and Y. Noack, Lead and zinc concentrations in household dust and toenails of the residents (Estarreja, Portugal): a source-pathway-fate model, *Environ. Sci.: Processes Impacts*, 2018, **20**, 1210–1224, DOI: [10.1039/c8em00211h](https://doi.org/10.1039/c8em00211h).

